

**LEFT-HANDED METAMATERIAL INCORPORATED WITH
MICROSTRIP ANTENNA**

HUDA BIN A. MAJID

UNIVERSITI TEKNOLOGI MALAYSIA

LEFT-HANDED METAMATERIAL INCORPORATED WITH MICROSTRIP
ANTENNA

HUDA BIN A. MAJID

A thesis submitted in fulfilment of the
requirements for the award of the degree of
Master of Engineering (Electrical)

Faculty of Electrical Engineering
Universiti Teknologi Malaysia

FEBRUARY 2010

*To my beloved father and mother for their understanding and support throughout my
quest in completing my Master*

ACKNOWLEDGEMENT

First of all, thanks to our creator for the continuous blessing and for giving me the strength and chances in completing this project.

Special thanks to my project supervisor, Associate Prof. Dr. Mohamad Kamal A. Rahim, for his guidance, support and helpful comments in doing this project.

My family deserves special mention for their constant support and for their role of being the driving force towards the success of my project. My friends deserve recognition for lending a helping hand when I need them. I would also like to thank the wonderful members of P18; Dr Thelaha Masri, Mr. Mohd Nazri A Karim, Mr. Osman Ayop, Mr Farid Zubir, Mrs. Maisarrah Abu, and my middle east friends; Mrs. Mai Abdul Rahim, Mr. Alii, Mr. Hassien, Mr. Hithem, Mr. Akram, Mr. Suhil and Mr. Kusay, who have also been extremely kind and helpful throughout my stay. “We don’t remember days, but we remember moments” and my moments with these guys are very fruitful during my study in UTM.

My sincere appreciation also goes to everyone whom I may not have mentioned above who have helped directly or indirectly in the completion of my project.

ABSTRACT

Left-handed metamaterial (LHM) is an artificial material where the permittivity and permeability are simultaneously negative at a certain range of frequency. One of the unique properties of the LHM is its negative refraction index which produces focusing effect to the wave propagating through the LHM. With this unique property, the LHM structures are used to increase the low gain of the microstrip antenna. In this work, an LHM structure consists of a modified split ring resonator (MSRR) and two capacitance loaded strip (CLS) is proposed. The MSRR has four slots in the middle of the structure which create wider range of negative permittivity and permeability. The MSRR exhibits negative permeability while the CLS exhibits negative permittivity. The well-known modified Nicolson-Ross-Wier (NRW) approach has been used to determine the values of permittivity and permeability. Parametric study on the parameters of the LHM has been carried out. The gap between the CLS – MSRR, the MSRR length and the CLS width show strong influence to the resonant frequency and the range of negative permittivity and permeability. A series of LHM structures are then incorporated with different antenna type such as single patch antenna, linear polarized 2x2 array patches antenna and circular polarized 2x2 array patches antenna at operating frequency of 2.4 GHz. The simulation and measurement results such as return loss, bandwidth, gain, half power beamwidth and radiation pattern are analyzed. The gain of the antennas increased upto 4 dB while the half power beamwidth decreased upto 37 % and became directional. The bandwidth of the antennas also increased upto 60 %.

ABSTRAK

Metabahan tangan kiri (LHM) adalah satu bahan buatan yang mana kebolehtelusan dan kebolehtelapan bahan itu adalah negatif pada julat frekuensi. Salah satu sifat unik LHM adalah indeks pembiasan negatif yang menghasilkan kesan fokus terhadap gelombang yang melalui LHM. Dengan sifat unik ini, LHM digunakan untuk mengatasi gandaan rendah pada antena mikrojalur. Struktur LHM yang terdiri daripada satu penyalun cincin terpisah (MSRR) yang telah dimodifikasi dan dua kapasitans jalur muatan (CLS) dicadangkan. MSRR mempunyai empat celahan di pertengahan struktur dan ia mewujudkan julat kebolehtelusan dan kebolehtelapan negatif yang lebih luas. MSRR mempamerkan kebolehtelapan negatif sementara CLS mempamerkan kebolehtelusan negatif. Pendekatan terkenal Nicolson-Ross-Wier (NRW) yang dimodifikasi telah digunakan untuk menentukan nilai kebolehtelusan dan kebolehtelapan. Kajian parametrik pada parameter LHM telah dilakukan. Lebar celahan antara CLS - MSRR, panjang MSRR dan lebar CLS menunjukkan pengaruh yang kuat kepada frekuensi resonans dan julat kebolehtelusan dan kebolehtelapan negatif. Satu rangkaian struktur LHM kemudiannya digabungkan dengan beberapa jenis antena seperti satu antena tampal, 2x2 antena tampal tatasusun linear berkutub dan 2x2 antena tampal tatasusun berkutub bulat beroperasi pada frekuensi 2.4 GHz. Hasil keputusan dari simulasi dan pengukuran seperti kehilangan balikan, lebarjalur, gandaan, lebaralur setengah kuasa dan corak sinaran dianalisis. Gandaan antena meningkat sehingga 4 dB manakala lebaralur setengah kuasa menurun sehingga 37 % dan menjadi terarah. Lebarjalur antena juga meningkat sehingga 60 %.

TABLE OF CONTENTS

CHAPTER	TITLE	PAGE
	DECLARATION	ii
	DEDICATION	iii
	ACKNOWLEDGMENT	iv
	ABSTRACT	v
	ABSTRAK	vi
	TABLE OF CONTENTS	vii
	LIST OF TABLES	xii
	LIST OF FIGURES	xv
	LIST OF SYMBOLS	xxvi
	LIST OF ABBREVIATIONS	xxviii
1	INTRODUCTION	
	1.1 Introduction	1
	1.2 Problem Statement	3
	1.3 The Scope of Research	3
	1.4 The Objective of Research	4
	1.5 Organisation of Thesis	4
2	LITERATURE REVIEW ON LEFT HANDED METAMATERIAL AND INCORPORATION WITH MICROSTRIP ANTENNA	
	2.1 Introduction	6
	2.2 Definition & Background of Left-Handed Metamaterial	6

2.3	History of Left-Handed Metamaterial (LHM)	7
2.4	Left-Handed Metamaterial Structure	8
2.4.1	Split Ring Resonator (SRR)	8
2.4.2	Capacitance Loaded Strip (CLS) and Thin Wire (TW)	9
2.5	Left-Handed Metamaterial Characteristics	11
2.5.1	Negative Refraction	11
2.5.2	Backward-wave Propagation	13
2.6	Method to Determine the Value of Permittivity and Permeability Using Modified Nicolson-Ross-Wier (NRW) Approach	16
2.7	Different Types of Left-Handed Metamaterial	19
2.7.1	Split Ring Structure	19
2.7.2	Symmetrical Ring Structure	20
2.7.3	Omega Structure	21
2.7.4	S-Shape Structure	22
2.7.5	Split Ring with Capacitance Loaded Strip Structure	23
2.7.6	Summary	24
2.8	LHM Application in Antenna Technology	25
2.8.1	Theoretical Investigation of a Circular Patch Antenna in the presence of a Left-Handed Medium	25
2.8.2	Metamaterial Enhanced Patch Antenna for WiMAX Application	28
2.8.3	A Study of Using the Double Negative Structure to Enhance the Gain of Rectangular Waveguide Antenna Array	31
2.8.4	Summary	34
2.9	Chapter Summary	35

3	DESIGN OF MICROSTRIP ANTENNA & LEFT-HANDED METAMATERIAL	
3.1	Introduction	35
3.2	Flow Chart of the Design Process	36
3.3	Methodology	38
3.4	LHM Design and Configuration	39
3.5	Boundary Condition for the Simulation Setup	42
3.6	Parametric Studies and Analysis of the Dependence between the Resonant Frequency and the Parameters of the Unit Cell	43
3.6.1	Varying the Gaps, G_1 and Width, W_2 of the MSRR	43
3.6.2	Varying the Gap between the MSRR and the CLS, G_2	45
3.6.3	Varying the Length of outer MSRR, L_2	46
3.6.4	Varying the Width of CLS, W_1	49
3.6.5	Parametric Studies Conclusion	50
3.7	Simulation of the LHM unit cells in Different Size of Air Gap	50
3.8	Microstrip Antenna Design	57
3.8.1	Single Patch Microstrip Antenna	57
3.8.2	Linear Polarized 2x2 Array Patch Microstrip Antenna	61
3.8.3	Circular Polarized 2x2 Array Patch Microstrip Antenna	65
3.9	Chapter Summary	69
4	SIMULATION AND MEASUREMENT OF MICROSTRIP ANTENNA INCORPATED WITH LEFT-HANDED METAMATERIAL	
4.1	Introduction	70
4.2	Simulation of Single Patch Microstrip Antenna Incorporated with LHM	70

4.3	Simulation of Linear Polarized 2 x 2 Array Patch Microstrip Antenna Incorporated with LHM	76
4.4	Simulation of Circular Polarized 2 x 2 Array Patch Microstrip Antenna Incorporated with LHM	78
4.5	Measurement Result	83
4.5.1	Measurement of Single Patch Microstrip Antenna Incorporated with LHM	85
4.5.2	Measurement of Single Linear Polarized 2 x 2 Array Patch Microstrip Antenna Incorporated with LHM	88
4.5.3	Measurement of Single Circular Polarized 2 x 2 Array Patch Microstrip Antenna Incorporated with LHM	92
4.6	Chapter Summary	96

5 ANALYSIS AND DISCUSSION

5.1	Introduction	97
5.2	Analysis and Discussion on Simulation of the Single Patch Microstrip Antenna Incorporated with LHM	97
5.2.1	E-field analysis in the present of LHM in front of the single patch microstrip antenna	100
5.3	Analysis and Discussion on Simulation of Linear Polarized 2x2 Array Patch Microstrip Antenna Incorporated with LHM	102
5.4	Analysis and Discussion on Simulation of Circular Polarized 2x2 Array Patch Microstrip Antenna Incorporated with LHM	105
5.5	Analysis and Discussion on Measurement of the Single Patch Microstrip Antenna Incorporated with LHM	108

5.6	Analysis and Discussion on Measurement of the Linear Polarized 2x2 Array Patch Microstrip Antenna Incorporated with LHM	113
5.7	Analysis and Discussion on Measurement of the Circular Polarized 2x2 Array Patch Microstrip Antenna Incorporated with LHM	117
5.8	Chapter Summary	124
6	CONCLUSION	
6.1	Overall Conclusion	126
6.2	Key Contribution	128
6.3	Future Work	129
	REFERENCES	130
	Appendices A - E	136 - 146

LIST OF TABLES

TABLE NO.	TITLE	PAGE
2.1	Comparison between five LHM designs	25
2.2	Comparison between three discussed papers	35
3.1	Comparison between different MSRR	40
3.2	Dimension of LHM	42
3.3	Correlation between frequency range of negative permittivity, ϵ_r and permeability, μ_r with gap, G_2	45
3.4	Correlation between gap, G_2 and length, L_1	46
3.5	Correlation between gap, G_2 and length, L_4	46
3.6	Correlation between frequency range of negative permittivity, ϵ_r and permeability, μ_r with length, L_2	47
3.7	Correlation between length, L_2 and length, L_3	48
3.8	Correlation between length, L_2 and length, L_1	48
3.9	Correlation between length, L_2 and length, L_4	48

3.10	Correlation between frequency range of negative permittivity, ϵ_r and permeability, μ_r with width, W_1	49
3.11	Comparison between 4 mm, 6 mm and 8 mm air gap	55
3.12	Comparison between unit cell with and without air gap	56
4.1	The results of the measured single patch microstrip antenna	86
4.2	The results of the measured single patch microstrip antenna incorporated with LHM	87
4.3	The results of the measured linear polarized 2x2 array patch microstrip antenna	89
4.4	The results of the measured linear polarized 2x2 array patch microstrip antenna incorporated with LHM	90
4.5	The results of the measured circular polarized 2x2 array patch microstrip antenna	92
4.6	The results of the measured circular polarized 2x2 array patch microstrip antenna incorporated with LHM	93
4.7	The results of the measured circular polarized 2x2 array patch microstrip antenna in cross polar position	94
4.8	The results of the measured circular polarized 2x2 array patch microstrip antenna incorporated with LHM in cross polar position	94

5.1	Comparison of the antenna's performance between single patch microstrip antenna with and without LHM	100
5.2	Comparison of the antenna's performance between linear polarized 2x2 array patch microstrip antenna with and without LHM	105
5.3	Comparison of the antenna's performance between circular polarized 2x2 array patch microstrip antenna with and without LHM	108
5.4	Comparison of the antenna's performance between single patch microstrip antenna with and without LHM	111
5.5	Comparison between simulated and measured single patch microstrip antenna incorporated with LHM	112
5.6	Comparison of the antenna's performance between linear polarized 2x2 array patch microstrip antenna with and without LHM	116
5.7	Comparison between simulated and measured linear polarized 2x2 array patch microstrip antenna incorporated with LHM	116
5.8	Comparison of the antenna's performance between circular polarized 2x2 array patch microstrip antenna with and without LHM	122
5.9	Comparison between simulated and measured circular polarized 2x2 array patch microstrip antenna incorporated with LHM	123

LIST OF FIGURES

FIGURE NO.	TITLE	PAGE
1.1	Different type of material	2
2.1	First experimental LHM structure	7
2.2	(a) Circular split ring resonator and (b) Square split ring resonator.	8
2.3	(a) Capacitance loaded strip (CLS) and (b) Thin wire (TW)	9
2.4	(a) TW (solid) and (b) CLS (dotted)	10
2.5	(a) The refracted wave in a RH Medium and (b) The refracted wave in a LH Medium	11
2.6	The negative refractive index obtained from experiment	12
2.7	The refocused wave after passing through the LHM Slab	12
2.8	(a) RH medium triad and (b) LH medium triad	15
2.9	Split ring resonator (SRR) and a single thin wire (TW)	20
2.10	(a) Value of permittivity and (b) Value of permeability	20

2.11	Symmetrical ring structure	21
2.12	(a) Value of permittivity and (b) Value of permeability	21
2.13	Omega shape structure	22
2.14	(a) Value of permittivity and (b) Value of permeability	22
2.15	S-Shape Structure	23
2.16	(a) Value of permittivity and (b) Value of permeability	23
2.17	Split ring resonator (SRR) and four capacitance loaded strip (CLS)	24
2.18	Value of permittivity and permeability	24
2.19	(a)Unit cell of the LHM consisting of SRR and electrical wires and (b) Dimensions of the SRR.	26
2.20	LH MTM incorporated with the circular patch antenna	26
2.21	Value of permittivity and permeability	26
2.22	(a) S_{11} of the patch antenna and (b) S_{11} of the patch antenna incorporated with LHM	27
2.23	(a) Radiation pattern of the patch antenna and (b) Radiation pattern of the patch antenna incorporated with LHM	28

2.24	Antenna incorporated with metamaterials (a) perspective view, (b) side view and (c) dimension of the unit cell	29
2.25	Measured return loss between ordinary patch antenna and the antenna incorporated with metamaterials (proposed antenna)	30
2.26	Measured (solid line) and simulated (dotted line) peak antenna gain across WiMAX 3.5 GHz band	30
2.27	Measured radiation patterns for E-plane (y-z plane) and H-plane (x-z plane)	31
2.28	DNG structure consist of SRR and SW	31
2.29	S_{11} and S_{21} results	32
2.30	Value of permittivity and permeability	32
2.31	Rectangular waveguide antenna incorporated with DNG structure	33
2.32	(a) Radiation pattern in E-plane and (b) Radiation pattern in H-plane	33
2.33	Fabricated rectangular waveguide antenna incorporated with DNG structure	34
2.34	(a) Radiation pattern in E-plane and (b) Radiation pattern in H-plane	34
3.1	Flow Chart of Designing LHM	37

3.2	(a) Side view of the LHM (b) Top view of the LHM and (c) Perspective view of the LHM proposed by Ziolkowski [10]	39
3.3	Proposed LHM structure	40
3.4	The dimension of the LHM structure	41
3.5	Boundary condition for simulation setup	42
3.6	Results of S_{11} and S_{21} of the LHM unit cell	44
3.7	Value of ϵ_r and μ_r	44
3.8	Correlation between gap, G_2 and resonant frequency	45
3.9	Correlation between length, L_2 and resonant frequency	47
3.10	Correlation between width, W_1 and resonant frequency	49
3.11	Simulation on single cell without air gap	51
3.12	Value of S_{11} and S_{21} of the single cell without air gap	51
3.13	Value of ϵ_r and μ_r of the single cell without air gap	52
3.14	Simulation on single cell with air gap	52
3.15	Value of S_{11} of the single cell with different size of air gap	53
3.16	Value of S_{21} of the single cell with different size of air gap	53

3.17	Value of ϵ_r of the single cell with different size of air gap	54
3.18	Value of μ_r of the single cell with different size of air gap	54
3.19	Value of ϵ_r , μ_r and refractive index for unit cell with 8 mm air gap	56
3.20	Layout of single patch microstrip antenna	58
3.21	Coaxial port coordinate	59
3.22	Return loss, S_{11} of the single patch microstrip antenna	59
3.23	3D radiation pattern at 2.4 GHz	60
3.24	(a) Polar plot of radiation pattern at 2.4 GHz in H-plane and (a) Polar plot of radiation pattern at 2.4 GHz in E-plane	61
3.25	Layout of the transmission line feeding technique	62
3.26	Layout of linear polarized 2x2 array microstrip patch antenna	63
3.27	Return loss, S_{11} of the 2x2 array patch microstrip antenna	63
3.28	3D radiation pattern at 2.4 GHz	64
3.29	(a) Polar plot of radiation pattern at 2.4 GHz in E-plane and (b) Polar plot of radiation pattern at 2.4 GHz in H-plane	65

3.30	Layout of Circular Polarized 2x2 Array Patch Microstrip Antenna	66
3.31	(a) E-field at 0^0 , (b) E-field at 90^0 , (c) E-field at 180^0 and (d) E-field at 360^0	67
3.32	Return loss, S_{11} of the 2x2 array patch circular polarized microstrip antenna	67
3.33	3D radiation pattern at 2.4 GHz	67
3.34	(a) Polar plot of radiation pattern at 2.4 GHz in E-plane and (b) Polar plot of radiation pattern at 2.4 GHz in H-plane	68
4.1	(a) Dimension of the microstrip antenna incorporated with LHM with three different views where (a) (b) front view, (c) side view and (d) back view	71
4.2	Return loss, S_{11}	72
4.3	(a) Simulated radiation patterns at 2.45 GHz, (b) Simulated radiation patterns at 2.48 GHz and (c) Simulated radiation patterns at 2.4 GHz	73
4.4	(a) Polar plot of the radiation pattern in H-plane at 2.4 GHz and (a) Polar plot of the radiation pattern in E-plane at 2.4 GHz	74
4.5	LHM structure	74
4.6	(a) Focusing effect of 12.5 mm gap and (b) Focusing effect of larger than 14.55 mm gap	75

4.7	Resonant frequency shift as the gap between the antenna and the LHM structure varies	75
4.8	Perspective view on the 2x2 array patch microstrip antenna incorporated with LHM	76
4.9	Return loss, S_{11}	77
4.10	(a) Simulated radiation patterns at 2.4 GHz and (b) Simulated radiation patterns at 2.45 GHz	77
4.11	(a) Polar plot of the radiation pattern in H-plane at 2.4 GHz and (b) Polar plot of the radiation pattern in E-plane at 2.4 GHz	78
4.12	Perspective view of the 2x2 array circular patch microstrip antenna	79
4.13	Return loss, S_{11}	80
4.14	Return loss altered as the gap between the antenna and the LHM varies	80
4.15	(a) Simulated radiation patterns at 2.35 GHz, (b) Simulated radiation patterns at 2.4 GHz and (c) Simulated radiation patterns at 2.45 GHz	82
4.16	(a) Polar plot of the radiation pattern in H-plane at 2.4 GHz and (b) Polar plot of the radiation pattern in E-plane at 2.4 GHz	82
4.17	(a) Measurement setup using network analyzer and (b) Layout of the measurement setup	84

4.18	(a) Measurement equipment for radiation pattern measurement (from left; signal generator, spectrum analyzer, antenna measurement rotator and rotator within an anechoic chamber) and (b) Layout of the measurement setup	84
4.19	(a) The fabricated single patch microstrip antenna and (b) the fabricated LHM	85
4.20	Perspective view of the single patch microstrip antenna incorporated with LHM	86
4.21	Measured radiation pattern of the single patch microstrip antenna	87
4.22	Measured radiation pattern of the single patch microstrip antenna with LHM	88
4.23	Perspective view of the 2x2 array patch microstrip antenna with and without LHM	89
4.24	Measured radiation pattern of the 2x2 array patch microstrip antenna	90
4.25	Measured radiation pattern of the 2x2 array patch microstrip antenna with LHM	91
4.26	Perspective view of the 2x2 array patch circular polarized microstrip antenna with and without LHM	92
4.27	Measured radiation pattern of the 2x2 array patch circular polarized microstrip antenna	95

4.28	Measured radiation pattern of the 2x2 array patch circular polarized microstrip antenna with LHM	95
5.1	Return loss, S_{11} of the single patch microstrip antenna incorporated with LHM	98
5.2	Radiation Patterns in E-plane	99
5.3	Radiation Patterns in H-plane	99
5.4	(a) Observation on E-field in E-plane for the single patch microstrip antenna and (b) Observation on E-field in E-plane for the single patch microstrip antenna incorporated with LHM	101
5.5	(a) Observation on E-field in H-plane for the single patch microstrip antenna and (b) Observation on E-field in H-plane for the single patch microstrip antenna incorporated with LHM	101
5.6	Return loss, S_{11} of the linear polarized 2x2 array microstrip patch antenna	102
5.7	(a) 3D radiation pattern of the linear polarized 2x2 array patch microstrip antenna incorporated with LHM and (b) 3D radiation pattern of the linear polarized 2x2 array patch microstrip antenna	103
5.8	Radiation pattern in E-plane	104
5.9	Radiation pattern in H-plane	104

5.10	Return loss, S_{11} of the circular polarized 2x2 array patch microstrip antenna	106
5.11	Radiation pattern in E-plane	106
5.12	Radiation pattern in H-plane	107
5.13	Return loss, S_{11} of the single patch microstrip antenna incorporated with and without LHM	109
5.14	Transmission coefficient, S_{21} of the single patch microstrip antenna incorporated with and without LHM	109
5.15	Radiation pattern in E-plane	110
5.16	Radiation pattern in H-plane	110
5.17	(a) Comparison between simulated and measured radiation patterns in E-plane and (b) Comparison between simulated and measured radiation patterns in H-plane	112
5.18	Return loss, S_{11} of the linear polarized 2x2 Array Patch Microstrip Antenna Incorporated with and without LHM	113
5.19	Transmission coefficient, S_{21} of the linear polarized 2x2 Array Patch Microstrip Antenna Incorporated with and without LHM	114
5.20	Radiation pattern in E-plane	115
5.21	Radiation pattern in H-plane	115

5.22	(a) Comparison between simulated and measured radiation patterns in E-plane and (b) Comparison between simulated and measured radiation patterns in H-plane	117
5.23	Return losses, S_{11} circular polarized 2x2 array patch microstrip antenna incorporated with and without LHM	118
5.24	Transmission coefficient, S_{21} in co-polar position of the circular polarized 2x2 array patch microstrip antenna incorporated with and without LHM	119
5.25	Transmission coefficient, S_{21} in cross-polar position of the circular polarized 2x2 array patch microstrip antenna incorporated with and without LHM	119
5.26	Co-polar radiation patterns in E-plane	120
5.27	Cross-polar radiation patterns in H-plane	120
5.28	Co-polar radiation patterns in E-plane	121
5.29	Cross-polar radiation patterns in H-plane	121
5.30	(a) Comparison between simulated and measured radiation patterns in E-plane and (b) Comparison between simulated and measured radiation patterns in H-plane	124

LIST OF SYMBOLS

E	-	Electric Field
H	-	Magnetic Field
D	-	Electric Flux Density
B	-	Magnetic Flux Density
ρ	-	Charge Density
S	-	Poynting Vector
P_0	-	Power Flow
ε	-	Permittivity
μ	-	Permeability
ε_r	-	Relative Permittivity
μ_r	-	Relative Permeability
n	-	Refractive Index
c	-	Speed of Light
ω	-	Radian Frequency
ω_p	-	Plasma Radian Frequency
k	-	Complex wavenumber
f	-	Frequency
λ	-	Wavelength
ξ	-	Damping Coefficient
Z	-	Impedance
β	-	Propagation Constant
σ	-	Conductivity of Metal
η	-	wave Impedance
T	-	Transmission Coefficient
Γ	-	Reflection Coefficient
v_p	-	Phase Velocity

f_{pm}	-	Magnetic Plasma Frequency
f_{pe}	-	Electric Plasma Frequency
S_{11}	-	Return Loss
S_{21}	-	Insertion loss
d	-	Thickness of the slab (LHM)

LIST OF ABBREVIATIONS

DNG	-	Double Negative
LHM	-	Left Handed Metamaterial
NRI	-	Negative Refractive Index
NRW	-	Nicolson-Ross-Weir
TW	-	Thin Wire
SRR	-	Split Ring Resonator
MSRR	-	Modified Split Ring Resonator
CLS	-	Capacitance Loaded Strip
FSS	-	Frequency Selective Surface

LIST OF APPENDICES

APPENDIX	TITLE	PAGE
A	List of Publications	136
B	Example of the Calculation on the modified NRW method using MathCAD	138
C	Refraction Index	141
D	Scaling the Dimension of the Left Handed Metamaterial Structure	145
E	Wet Etching Process	146

CHAPTER 1

INTRODUCTION

1.1 Introduction

Recently, there have been frequent study and research by researchers around the world regarding the left handed metamaterial that contradict with a lot of the physics law. The unusual characteristics of these materials have yet to be found in any natural material and are considered as a new material studied in the 21st century.

Left-handed metamaterial (LHM) is an artificial material (periodic metallic structure) where the permeability and permittivity were simultaneously negative at a certain range of frequency [1]. Before venturing deeper into this topic, a brief look into the material terminology would help in understanding this peculiar artificial material. Figure 1.1 shows the terminology of the materials.

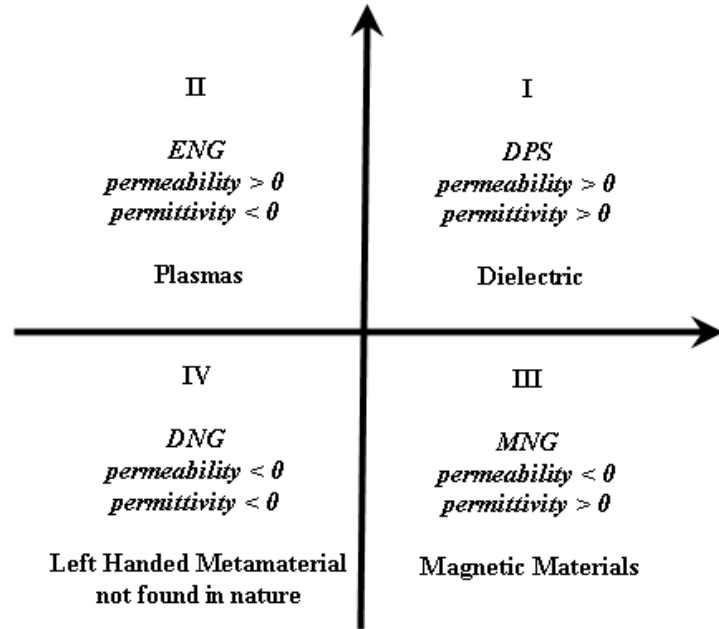


Figure 1.1: Different type of material

From the figure, the material terminology is divided into 4 groups. Group I shows the Double Positive (DPS) material which have positive value of permittivity and permeability. Almost all existing materials are DPS material and one of the examples is dielectric. For group II, Epsilon Negative (ENG) material has only permeability in positive value but the permittivity is negative. On the other hand, group III represents Miu Negative (MNG) material which is opposite of ENG material where the value of permittivity is positive and the value of permeability is negative. Lastly, the group IV shows the Double Negative (DNG) material and also known as Left Handed Metamaterial (LHM). This material has both permittivity and permeability in negative value. The works in this thesis focus on group IV material where the value of the permittivity and permeability are negative.

Left Handed Metamaterial has a few unique and unusual properties due to negative value permittivity and permeability of the structure itself. Therefore, a fair amount of explanation has to be presented in order to showcase this newly discovered material. Their properties are discussed in chapter 2. One of the unique properties of Left Handed Metamaterial is negative refraction which will produce the focusing effect. With this property, LHM will be used to focus the radiation of an antenna thus should increased the gain of the antenna.

1.2 Problem Statement

The study of the Left-Handed Metamaterial is carried out due to escalating interest in this unique material and its immense potential in various applications.

The material with negative value of permittivity and permeability is not found in nature. By applying the concept, theory and design of the Left-Handed Metamaterial, the material with negative value of permittivity and permeability can be created artificially.

Microstrip antenna suffered low gain. A common technique to overcome this drawback is using array of patch antenna. However, this technique has drawbacks which are high feed network losses and produce mutual coupling [2]. Another method to overcome this disadvantage is by using the Left Handed Metamaterial. The integration of the Left Handed Metamaterial with the microstrip antenna will increase the gain of the microstrip antenna. With this feature, the antenna that integrates with the Left Handed Metamaterial structure can be used for longer range point to point or point to multipoint wireless communication or to extend wireless coverage.

1.3 Scope of Research

The main scopes of the research are:

- i. Study the Left-Handed Metamaterial and microstrip antennas.
- ii. Design, simulate and analyze Left-Handed Metamaterial using Computer Simulation Technology (CST) CAD tools.
- iii. Simulate the Left-Handed Metamaterial incorporate with the single patch, 2x2 array patch and circular polarized 2x2 array patch microstrip antenna.
- iv. Measurement the Left-Handed Metamaterial incorporate with the single patch, 2x2 array patch and circular polarized 2x2 array patch microstrip antenna.

- v. Analyze and compare the results between simulation and measurement.
- vi. Thesis write up.

1.4 Objective of Research

The main objectives of this research are:

- i. To study, design, simulate and analyze the new structure of Left-Handed Metamaterial.
- ii. To simulate, fabricate and measure the Left-Handed Metamaterial incorporated with the single patch microstrip antenna, 2x2 array patch microstrip antenna and 2x2 array circular polarized patch microstrip antenna.
- iii. To compare and analyze the behavior and properties of the microstrip antennas incorporate with Left Handed Metamaterial.

1.5 Organisation of Thesis

Chapter 1 discusses the brief introduction of Left Handed Metamaterial, the problem statement, the objective and scope of the research as well as the organization of the thesis.

Chapter 2 explains the basic concepts and theories of the Left Handed Metamaterial. The unique properties of this material are elaborated thoroughly in this chapter.

Chapter 3 discusses on the design of the Left Handed Metamaterial using Computer Simulation Technology (CST) and MathCAD software. For the completeness of the thesis, the design equation of the single patch microstrip

antenna, 2x2 array patch microstrip antenna and 2x2 array patch circular polarized microstrip antenna are also presented.

The simulation and measurement results of the Left Handed Metamaterial incorporated with the antenna are discusses in Chapter 4.

In Chapter 5, the results of the antennas with and without Left Handed Metamaterial are analyzed in terms of return loss, gain, directivity, half power beam width and others antenna's parameters. The results are presented in a form of tables and graphs.

Lastly, Chapter 6 concludes the finding of the project, key contributions and recommendations for future research.

In addition, the list of references and appendices were listed at the end of this thesis.